



Reversible information hiding scheme based on interpolation and histogram shift for medical images

Fang Ren^{1,2} · Yuge Liu^{1,2}  · Xing Zhang¹ · Qiang Li¹

Received: 2 August 2022 / Revised: 2 October 2022 / Accepted: 10 December 2022 /
Published online: 2 February 2023

© The Author(s), under exclusive licence to Springer Science+Business Media, LLC, part of Springer Nature 2023

Abstract

Medical imaging and information management systems require transmission and storage of medical images over the Internet. Many reversible information hiding schemes for image have been proposed to ensure security and availability. In order to avoid the risk of medical information leakage and the medical image distortion, a reversible information hiding scheme based on interpolation and histogram shift for medical images has been proposed in this paper. The proposed adaptive interpolation between neighbor pixels (AIA) technique is used to obtain seed and non-seed pixels, which ensures the reversibility of the scheme while balancing the embedding capacity and the quality of marked image. Then, the image is divided into the region of interest (ROI) and the region of non-interest (NROI). Sensitive information such as electronic patient records (EPR) and electronic signatures of medical images are embedded as secret information. In the ROI, the corresponding bit histogram shift repeated embedding method (CBHSR) is adopted for embedding information to effectively avoid the problem of image distortion caused by histogram stretching. Experimental results show that algorithm not only has high embedding capacity, but also keeps the peak signal-to-noise ratio above 50dB, visual information fidelity and structural similarity above 0.99, which has good subjective and objective image quality.

✉ Yuge Liu
1842730383@qq.com

Fang Ren
76487690@qq.com

Xing Zhang
3489354626@qq.com

Qiang Li
liq_97@163.com

¹ School of Cyberspace Security, Xi'an University of Posts and Telecommunications, Xi'an, 710121, Shaanxi, China

² National Engineering Laboratory for Wireless Security, Xi'an University of Posts and Telecommunications, Xi'an, 710121, Shaanxi, China

Keywords Reversible information hiding · Medical image · Interpolation expansion · Histogram shift · Image segmentation · Privacy protection

1 Introduction

With the continuous development of society, hospitals are constantly building and improving medical information management systems, a variety of medical information is developing in the direction of digital. The rapid development of Internet technology and multimedia technology has provided new technical means for telemedicine, remote diagnosis and surgery. Although digital medical information is convenient to store and transmit, saving time and cost of transmission, it can easily be illegally copied and tampered with, which leads to the leakage of patients' privacy and even misdiagnosis. Medical images, as one of the important bases for doctors to diagnose diseases, put forward very strict requirements on the image quality. Any slight distortion can cause misdiagnosis and even serious medical accidents. How to address the security of medical information in network environment is a practical problem that must be solved in the process of medical information system construction.

In order to ensure the confidentiality, reliability and usability of medical images, researchers focus on reversible information hiding technology. As we all know, encryption technology can be used to guarantee the security of image content. Different from traditional cryptography, information hiding technology [17] is utilized the redundancy of human perception system and secret information is embedded into the cover information without being perceived, which can be used in copyright protection, image authentication, operation tracking and other fields. Compared with the traditional cryptography, the information hiding technology has the imperceptible characteristic, thus the information embedding is invisible. Reversible information hiding technology is an important branch of information hiding technology, because of its reversible characteristics, it has become a hot research topic. Compared with the traditional information hiding technology, the reversible information hiding technology can not only correctly extract the secret information, but also recover the cover image without damage, which is of great practical significance for medical, military, legal and other fields with high requirements on image quality.

For fear of the problem of information leakage in medical field, this paper proposes a reversible information hiding scheme based on interpolation and histogram shift for medical images. In data sharing, like telemedicine, sensitive information such as personal information (name, age, electronic medical records, etc.), medical insurance and social security, and electronic signature of medical images are easily leaked, which will bring serious consequences to patients and hospitals, as well as negative impacts on the society. The patients' personal information and hospital identification information (logo) are embedded in the medical image by using the proposed scheme. On the one hand, the privacy of patients is protected, and on the other hand, the ownership of medical images is maintained. Doctors' diagnostic information can also be embedded in medical images to facilitate efficient delivery of diagnostic protocols when patients change teams, thus better facilitating medical consultation, diagnosis and treatment. To some extent, it will also become an effective evidence to deal with medical malpractice disputes. In this still-COVID-19 era, nucleic acid reports have become our passport to free and secure access to places, but they are often sent as screenshots, which greatly reduces security. The proposed method is used to embed personal information, test results and official watermark into the picture of the nucleic acid

report, which is not only easy to detect tampers, but also indicates that the report has been modified if the extracted information is incomplete, and then the authenticity of the nucleic acid report can be identified.

The application of reversible information hiding for medical images has been experienced for a long time. A simple diagram is shown in Fig. 1.

At present, there are three basic techniques for reversible information hiding: difference expansion (DE), histogram shift (HS) and prediction error expansion (PEE). Shi et al. [31] firstly proposed a reversible information hiding technique. Tian et al. [35] proposed a reversible data hiding scheme based on difference expansion, in which secret information is hidden by expanding the difference between a pair of pixels. We applied this technique to our scheme. Ni et al. [27] proposed a reversible information hiding scheme based on histogram, in which the secret information was embedded at the histogram peak bin of the cover image. Thodi et al. [34] proposed a reversible watermarking scheme based on prediction error, embedding secret information into the pixel prediction error calculated by the extended prediction algorithm. Sachnev et al. [29] had shown that rhombus predicted pixels were expanded to embed the data. Adaptive embedding is one another technique which when combined with PEE improves the performance of embedding. Based on the above research, researchers continue to optimize and improve the scheme, especially to seek the balance between embedding capacity and embedding quality, then propose schemes with better performance.

Other techniques have been used by researchers to combine with basic techniques for reversible information hiding in medicine. Image interpolation is used to ensure the reversibility of the cover image. In image interpolation, the cover image with a size of $2M \times 2N$ is obtained using an image with a size of $M \times N$. There are some classical image interpolation techniques [3] : Nearest neighbor interpolation (Nearest), bilinear interpolation (Bilinear) and bicubic interpolation (Bicubic). In addition, interpolation techniques commonly used for reversible information hiding are proposed, such as neighbor

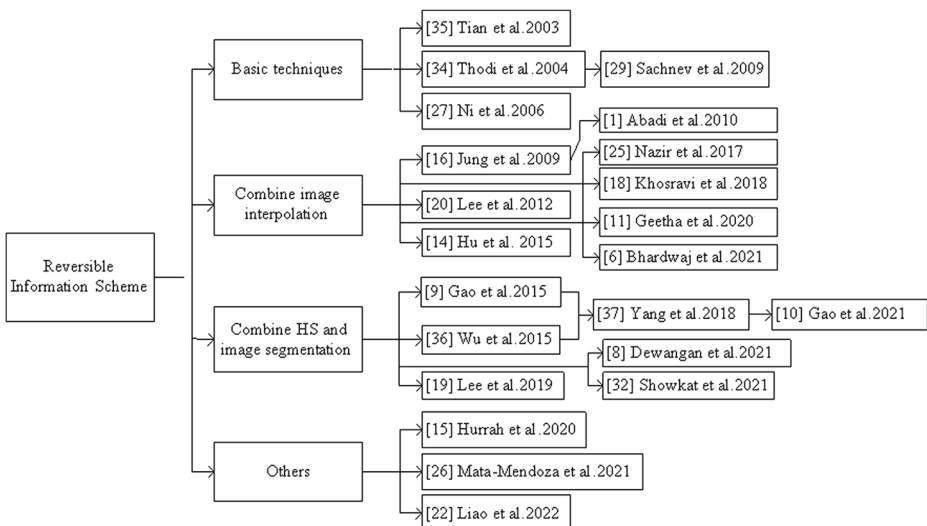


Fig. 1 Simple illustration of the literature review

mean value interpolation (NMI), neighbor pixel interpolation (INP) and maximizing neighbor pixel difference interpolation (IMPI). Jung et al. [16] proposed the first NMI-based reversible data scheme, which used seed pixels and non-seed pixels, with lower time complexity and higher computational speed. However, since boundary pixels were not used, the embedding capacity is relatively low. Abadi et al. [1] to increase the payload by using histogram modification technique, did a further modification to Jung. Lee et al. [20] used INP in the reversible data hiding scheme, which effectively improved the embedding capacity and had better image quality than NMI. Under the condition of ensuring the image quality, Hu et al. [14] proposed to maximize the difference between neighbor pixels to increase the embedded capacity, and the performance of the scheme was further improved. Nazir et al. [25] proposed a high-capacity reversible medical image data hiding scheme based on pixel repetition method (PRM) and mixed edge detection, which used the concept of image interpolation to hide the electronic medical records in medical images. Different from NMI, NPI, etc., PRM directly assigned the pixel values of the seed pixels to the neighbor non-seed pixels without using an algebraic method. The scheme used minimal computation, but its security needed to be considered. Khosravi et al. [18] proposed a lossless data hiding scheme for medical images based on reversible interpolation watermark error histogram calculation and greedy weight quartile interpolation. In this scheme, the greedy weight of the quartet interpolation was used to calculate the error histogram, and an adaptive linear least mean square error estimation (ALMMSE) interpolation algorithm was designed by changing the weight and optimizing the coefficient selection. The algorithm is suitable for gray and color medical images and can also be used for multi-layer embedding. Although the scheme has high image quality and embedding capacity, its time cost is high. Geetha et al. [11] proposed that the diamond-shaped mean interpolation technique was used to predict the interpolation points in the cover image, and the data related to patient diagnosis was embedded into the medical image as secret information, and the embedded checksum was used for tamper detection and content authentication. Although the image quality of the scheme is very good, its calculation amount is very large. The enhanced dual-image separable data hiding scheme proposed by Rupali Bhardwaj in the literature [6] utilizes the average pixel repetition (APR) for image interpolation, and its security is improved due to the encryption involved. The scheme relies on complex mathematical theory and double image, so it is difficult in practical application. We propose a new image interpolation method AIA, which largely ensures the embedding quality and capacity under the premise of satisfying the reversibility and has good applicability in the proposed scheme.

The reversible information hiding scheme for medical image based on histogram shift and image segmentation is an important research direction. Two reversible data hiding schemes with image contrast enhancement by histogram shift were achieved in [9] and [36]. They have some limitations. Firstly, two methods only applied histogram shifting (HS) scheme to select two highest bins of image histogram for data hiding and repeated this process until embedded all secret data. Hence, they caused the overflow and underflow due to use of the histogram shifting and they solved this case by using preprocessing handle. However, preprocessing handle could lead to new distortion of the marked image. Second, two methods only enhanced contrast in the global spatial domain but do not specifically for the image's ROI region, so they preferentially enhanced the background region of the medical images. Medical images have a large number of smooth regions. In the actual diagnosis, doctors are mostly concerned with the degree of change of the lesion location. Based on this point, the researchers proposed to divide medical image into ROI and NROI. The NROI is also called background region in some articles. Information hiding schemes based

on region segmentation have also been continuously developed. Lee et al. [19] proposed an adaptive reversible watermarking algorithm, which segmented the ROI and the background region, extended the estimation error of neighbor pixels to embed the watermark, and used error pre-compensation technology to solve the inherent overflow and underflow problems. But its embedding capacity needs to be strengthened. Dewangan et al. [8] analyzed the real-time performance in medical image applications and proposed a security solution for medical image recovery. The embedded block is selected in the ROI to irregularly estimate the ROI of the medical image, thus preserving the basic information of the image. Secure image communication was achieved by preserving the ROI that cover sensitive medical diagnostic information. But the embedding capacity of the scheme needs to be further improved. Combined with the regionalization and contrast enhancement scheme, Yang et al. [37] proposed a large-capacity reversible medical image data hiding scheme based on contrast enhancement of the ROI. In the scheme, an adaptive threshold detector was used for image region segmentation, and the contrast was enhanced by stretching the histogram of the ROI, and the histogram was embedded cyclically. The experimental results show that the proposed scheme can effectively improve the quality of medical images both in low and high embedding rate. However, since the histogram of ROI is stretched, the contrast of the marked image is much higher than that of the original image, and its imperceptibility is damaged to some extent. On this basis, Gao et al. [10] further improved the performance of the algorithm by adaptively selecting the ROI stretch range. But the visual changes in the marked images are also apparent. Showkat et al. [32] proposed a reversible data hiding scheme for medical images with contrast enhancement to add the tamper detection function. The goal is not to increase peak signal-to-noise ratio and embedding capacity, so these aspects need to be improved. In the above scheme, embedding information directly in the stretched histogram inevitably leads to a significant increase in image contrast and destroys the imperceptibility of information hiding requirements. We use the histogram stretching method that causes contrast distortion as a tool for position selection. By flexibly selecting the location of information embedding in the ROI, the security of secret information embedding and extraction can be improved on the one hand, and the good quality of the marked image can be guaranteed on the other hand, especially effectively avoiding the damage of imperceptibility.

The application of reversible information hiding technology in medical images is not limited to grayscale images and single images. Liao et al. [21, 22, 33] put their research into color images and multiple images to improve safety. Also, the application is not only limited to the spatial domain. At present, some researchers have turned their fields of view to the transform domain and the encryption domain, and they are in the initial stage. Bamal et al. using walsh-slantlet transform for Dual hybrid medical images. For some preliminary results, please refer to the literature [4, 5, 15, 17, 23, 26, 30] for details. The transformation domain is not involved in this paper. We will study these in the future.

In this paper, considering the characteristics of medical images, combined with interpolation technology, segmentation technology and histogram shift technology, a reversible information hiding scheme based on interpolation and histogram shift for medical images is proposed. The proposed scheme uses Otsu's method [28] for image segmentation, and the prediction error expansion [35] is used for RONI information embedding. The innovations of the proposed algorithm mainly include:

- (1) A new adaptive interpolation algorithm between neighbor pixels (AIA) is proposed, which is superior to most existing interpolation methods in comprehensive performance.

- (2) A corresponding bit histogram shift repeat embedding/extraction method (CBHSR) is proposed to improve the embedding quality while ensuring the embedding capacity.
- (3) An improved RLE compression algorithm is proposed to embed the location map more effectively.
- (4) The original image is recovered by using the seed pixels, and the algorithm complexity is low.

The structure of this paper is as follows. Section 2 presents the details of the proposed scheme. Section 3 discusses the experimental results and presents the performance analysis. Section 4 is a summary.

2 The proposed scheme

The proposed reversible information hiding scheme based on interpolation and histogram shift for medical images includes five stages: image interpolation, image segmentation, reversible data hiding based on ROI, reversible data hiding based on NROI, and data extraction and image recovery.

2.1 Adaptive interpolation expansion technique between neighbor pixel

The cover image is obtained by preprocess that input image. Assuming that the size of the input image is $M \times N$, the cover image with a size of $2M \times 2N$ is obtained by adaptively selecting and rounding and performing interpolation expansion by using the neighbor pixels. In this paper, the pixel of the input image is called seed pixel, and the pixel obtained by interpolation is non-seed pixel, in which the seed pixels remain unchanged during the embedding process. The input image is represented by A and the cover image is represented by I . The image interpolation is performed according to (1) to (4):

$$I(2i, 2j) = A(i, j). \quad (1)$$

$$I(2i, 2j+1) = \begin{cases} \left\lfloor \frac{A(i, j) + A(i, j+1)}{2} \right\rfloor, & A(i, j) < A(i, j+1) \\ \left\lceil \frac{A(i, j) + A(i, j+1)}{2} \right\rceil, & \text{others} \end{cases} \quad (2)$$

$$I(2i+1, 2j) = \begin{cases} \left\lfloor \frac{A(i, j) + A(i+1, j)}{2} \right\rfloor, & A(i, j) < A(i+1, j) \\ \left\lceil \frac{A(i, j) + A(i+1, j)}{2} \right\rceil, & \text{others} \end{cases} \quad (3)$$

$$I(2i+1, 2j+1) = \begin{cases} \left\lfloor \frac{A(i, j) + A(i+1, j+1)}{2} \right\rfloor, & A(i, j) < A(i+1, j+1) \\ \left\lceil \frac{A(i, j) + A(i+1, j+1)}{2} \right\rceil, & \text{others} \end{cases} \quad (4)$$

Where, $i=0, 1, \dots, M-1, j=0, 1, \dots, N-1$. The pixel values of the last row and last column of the cover image are equal to those of the penultimate row and penultimate column

A simple AIA is shown in Fig. 2. The input image with the size of 2×2 is expanded to 4×4 , and one seed pixel can get three non-seed pixels.

2.2 Corresponding bit histogram shift repeat embedding method

The CBHSR is put forward on the basis of histogram shifting technique [37]. The proposed technology integrates histogram shift technology with the characteristics of medical images

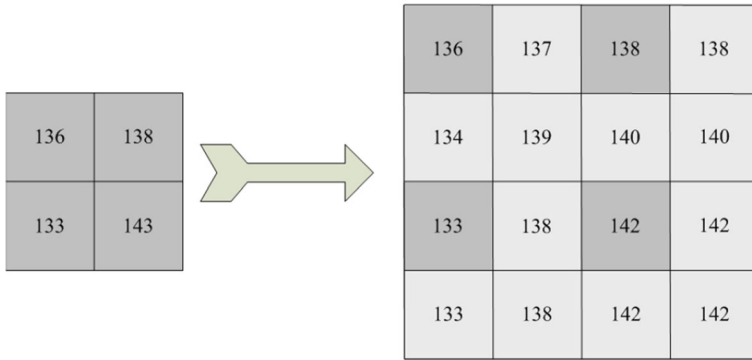


Fig. 2 Example of AIA

and avoids the problem of image contrast distortion caused by paper [37]. The concrete process is as follows:

- (1) Construct the histogram H and stretched histogram SH of the image. Assuming that the pixel value range of image histogram is $[H_{min}, H_{max}]$, then, the stretched histogram range is $[L_{min}, L_{max}]$ obtained by (5), where round indicates that the round rule is adopted. The pixel value range after stretching generally is $[0,255]$.

$$SH(x, y) = round \left[(L_{max} - L_{min}) \times \frac{H(x, y) - H_{min}}{H_{max} - H_{min}} + L_{min} \right] \quad (5)$$

- (2) Find the peak bin which its neighbor bin is absent in the SH and embed the secret information in the corresponding position of the H . Note that if the pixel values in the SH have no corresponding pixel values in the H , the peak bin will not be used. Record the available peak bin in the stretched histogram as set S . When there are the number of n available peak bin, the set S can be expressed as $\{s_1, s_2, \dots, s_n\}$. The gray value of peak bin is embedded into the next round of embedding process together with the secret information, and the last round of peak bin value is embedded into the square region. Although SH changes with H embedding information, it does not actually embed information itself. Simply put, the embedding process uses the stretch histogram as a tool to select the embedding location.
- (3) When embedding information, the H and SH are divided into left and right parts. When that secret information is '1' and the peak bin which with absent right neighbor bin is in the left half of SH , the right shift is performed in the corresponding pixel bin of H . When secret information is '1' and the peak bin which with absent left neighbor bin is in the right half of SH , the left shift is performed in the corresponding pixel bin of H . When the secret information is '0', the pixel bin of H does not change. As shown in (6), where k_1 is the peak bin of the H , k_2 is the peak bin of the SH , and k' is the peak bin of image histogram after the secret information is embedded.

$$k' = \begin{cases} k_1 + b_i, & k_2 \in [0, 126] \text{ and } SH(k_2 + 1) = 0 \\ k_1 - b_i, & k_2 \in [129, 255] \text{ and } SH(k_2 - 1) = 0, b_i = 0 \text{ or } 1 \\ k_1 & k_2 \notin S \end{cases} \quad (6)$$

- (4) Repeat (2) and (3) until there is no peak bin that satisfies the condition.

- (5) The extraction and recovery process are the inverse of the process described above. The ROI is recovered repeatedly as (7), where k'_2 is modified k_2 .

$$k = \begin{cases} k' - 1, & k'_2 \in [0, 126] \text{ and } k'_2 = k_2 + 1 \\ k' + 1, & k'_2 \in [129, 255] \text{ and } k'_2 = k_2 - 1 \\ k', & \text{others} \end{cases} \tag{7}$$

And secret information are extracted repeatedly as:

$$b_i = \begin{cases} 1, & k'_2 \in [0, 126] \text{ and } k'_2 = k_2 + 1 \\ 1, & k'_2 \in [129, 255] \text{ and } k'_2 = k_2 - 1 \\ 0, & k' = k_1 \end{cases} \tag{8}$$

A simple example of the CBHSR are shown in Figs. 3, 4 and 5.

The concrete embedding process is shown in Fig. 4. The left sub-figure is embedding position selection process by using the *SH*. The right sub-figure is the information embedding process of the *H*. Stretch the range of pixel values from [3,8] to [1,10] for information embedding. At first round, the histogram have pixel bins of $k_1 \in (3, 4, 7, 8)$ and the stretched histogram have pixel bins of $k_2 \in (1, 3, 8, 10)$. Finding the peak bin of the *SH*, namely, $SH(3)=20$ which bin belongs to [1,4], and its right neighbor bin is absent. Hence, we can embed 20bits information into $H(4)$. Here, we suppose the probability of the '1' and '0' in secret data are all 0.5, then $H(4)= H(5)=10$ and $SH(3)=SH(4)=10$. At second round, the peak bin of the modified *SH* is $SH(8)=16$ which bin belongs to [7,10] and its left neighbor bin is absent, then 16bits data are embedded into $H(7)$, so $H(7)= H(6)=8$ and $SH(8)= SH(7)=8$. At third round, the peak bin of the modified *SH* is $SH(1)=10$ which bin belongs to [1,4] and its right neighbor bin is absent, then 10bits data are embedded into $H(3)$, so $H(3)= H(4)=5$ and $SH(1)= SH(2)=5$. At fourth round, $SH(3)$ has no absent left neighbor bin, $SH(4)$ and $SH(7)$ have no corresponding bits in the *H*, so they are not used. Thus, the peak bin of the modified *SH* is $SH(10)=8$ which bin belongs to [7,10] and its left neighbor bin is absent, then 8bits information are embedded into $H(8)$, so $H(8)= H(7)=4$ and $SH(10)= SH(9)=4$. All selected bins are filled in and 54bits maximum information are embedded into the selected bins. As shown in right sub-figure of Fig. 3, the first row is the embedding result of the *H* which will be a part of marked image histogram and the second row is the embedding result of the *SH*. It's worth noting that the gray value of peak bin need be embedded into next round by using 8 bits and last round's peak bin will be saved.

The concrete extraction process is shown in Fig. 5. The left sub-figure is the process of extracting information from the marked image histogram. The right sub-figure is the process

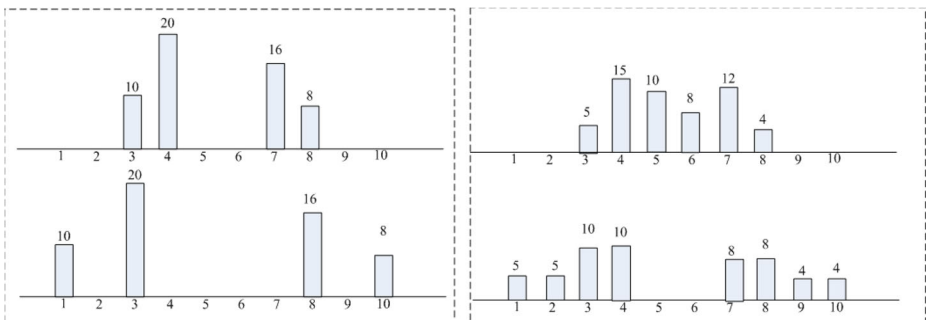


Fig. 3 Examples of inputs and results embedded by CBHSR

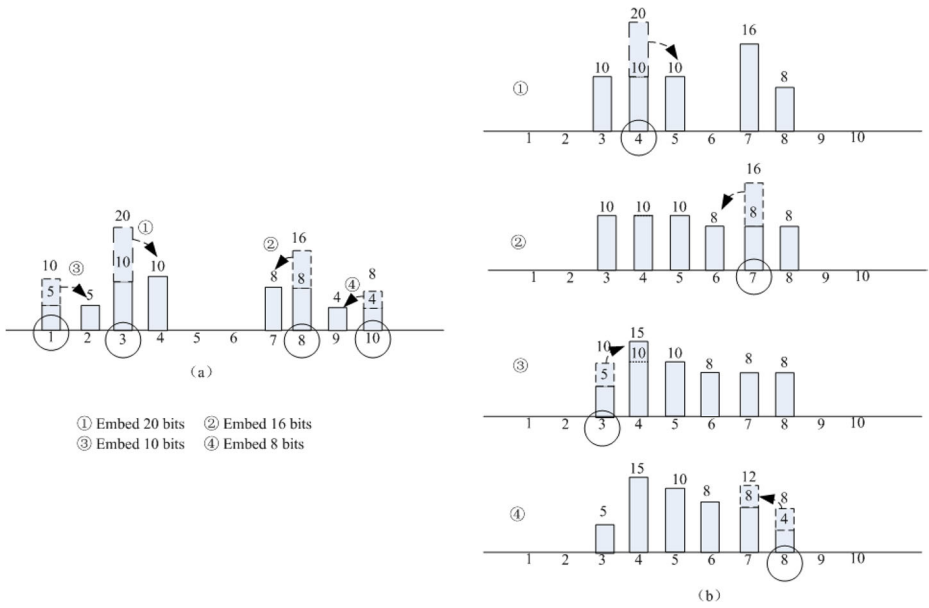


Fig. 4 Examples of embed process by CBHSR

of extracting information from the marked image histogram. At first round, last round's peak bin is SH(10) which bin belongs to [7,10] and its left neighbor bin is SH(9)=4, then 8bits of embedded information are extracted from H(8) and H(7). Repeated four extraction

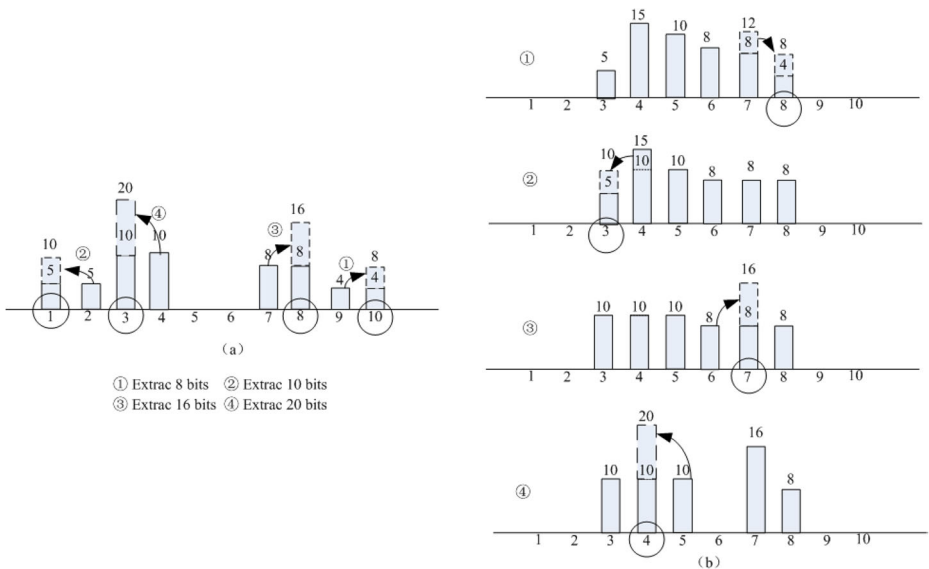


Fig. 5 Examples of extract process by CBHSR

rounds until the secret information is extracted completely. As shown in left sub-figure of Fig. 3, the first row of recover histogram is the H and the second row is the SH .

2.3 Embedding algorithm

The embedding algorithm diagram of the proposed scheme is shown in Fig. 6.

Step1 Image expansion

The cover image I with the size of $2M \times 2N$ can be obtained from the input image A with the size of $M \times N$ by AIA. The concrete steps of interpolation expansion are

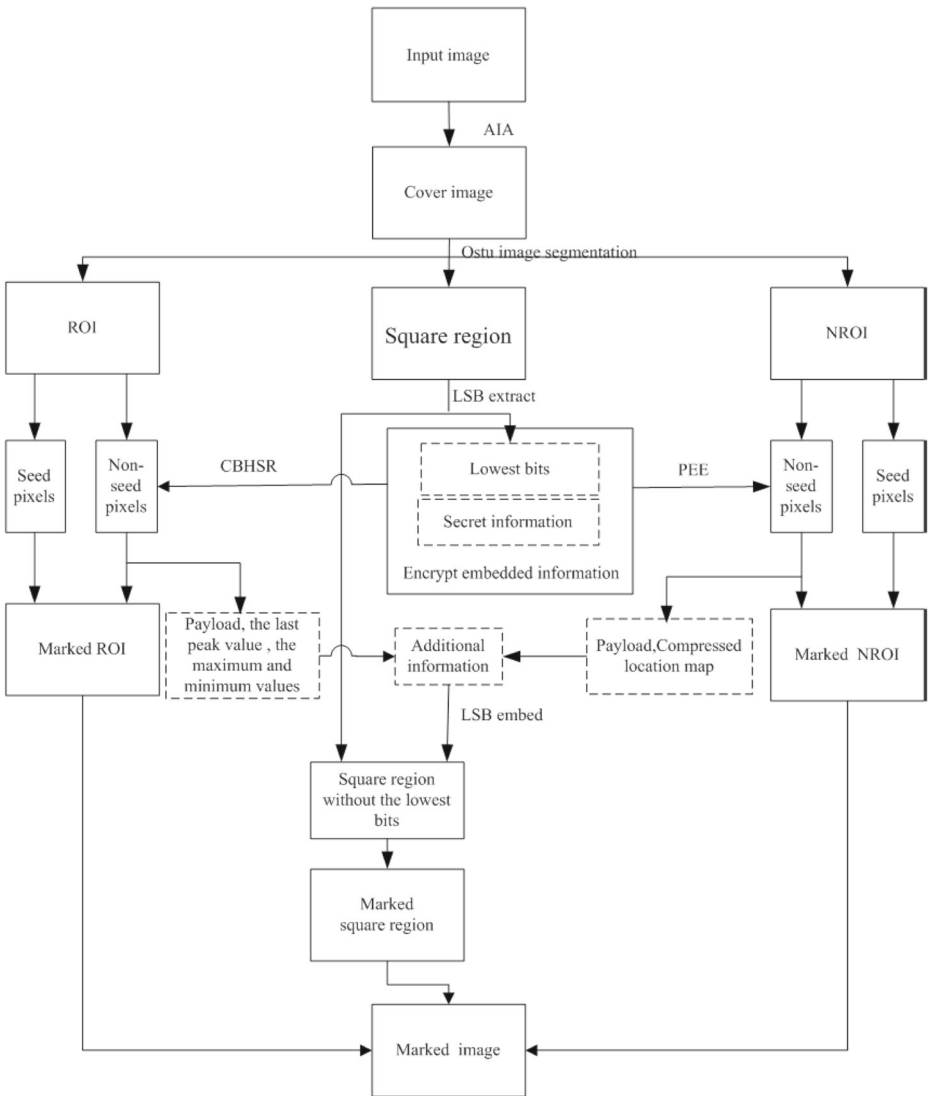


Fig. 6 Embedding algorithm diagram of the proposed scheme

described in Section 2.1. The pixels of input image are seed pixels, and the expanded pixels are non-seed pixels.

Step2 Image segmentation

Considering the characteristics of medical images, the cover image is divided into the ROI, the NROI and the square region. The ROI is the central region of image that contains important information that is helpful for accurate diagnosis. The NROI is a region containing information that is not useful in diagnosis. The square region is a fixed-size area around the medical image, like Fig. 7, where h is a fixed value in advance.

Otsu segmentation method [28] is adopted in this paper, a maximum class spacing method, to segment the image by finding the best threshold. When the seed pixel $I(2i, 2j)$ is divided into ROI, three non-seed pixels $I(2i + 1, 2j)$, $I(2i, 2j + 1)$ and $I(2i + 1, 2j + 1)$ by seed pixel expansion also belong to ROI.

Step3 Embedded information generation

The square region is preprocessed, and the the lowest bit and the pixels with lowest bit vacancy are obtained by LSB extraction. The lowest bits of pixels in the square area are connected to the secret information as embedded information for cover recovery. The secret information includes private information such as patient information and diagnosis information. Encrypt embedded information to get encrypted embedded information B .

Step4 ROI information embedding

The encrypted embedded information B is embedded into the non-seed pixels of the ROI according to CBHSR described in Section 2.2, and the seed pixels remain unchanged, thus obtaining the marked ROI. In order to correctly extract information and restore images, it is necessary to save ROI payload size, the last peak bin of ROI, the maximum and minimum values of cover ROI pixels as additional information.

Step5 NROI information embedding

The rest of the information in B is embedded into the non-seed pixels of the NROI according to the prediction error expansion method, and the seed pixels are kept unchanged to obtain the marked NROI. To avoid pixel overflow, the location map is used. The process of prediction error expansion:

- (1) Predictor: The average value of the left and right neighbor pixels of the current pixel x_i is calculated as the predicted value x'_i , as shown in Fig. 8 for 1×3 image block composed of non-seed pixels. The mathematical expression of the predictor is (9):

$$x'_i = \frac{x_{i+1} + x_{i-1}}{2} \tag{9}$$

Fig. 7 Example of the square region

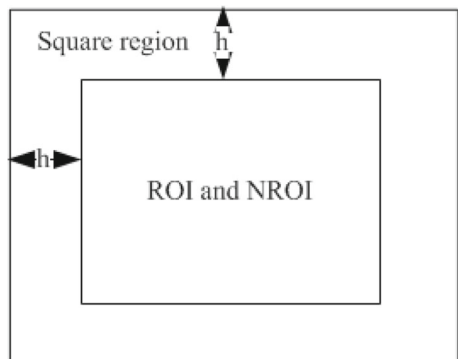
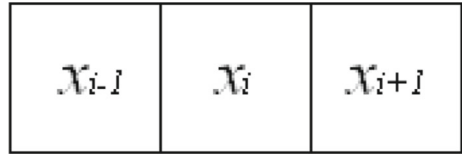


Fig. 8 Example of predictor region



(2) Prediction error:

$$e_i = x_i - x'_i \tag{10}$$

(3) The prediction error is expanded and embedded information, where T is used to indicate the range of the used prediction error value.

$$e'_i = \begin{cases} 2e_i + b & e_i \in [-T, T) \\ e_i + T & e_i \in [T, +\infty) \\ e_i - T & e_i \in (-\infty, T] \end{cases} \tag{11}$$

(4) Modify pixel value:

$$x''_i = x'_i + e'_i \tag{12}$$

In order to correctly extract information and restore the cover image, NROI location map and payload are saved as additional information. NROI location map M is a binary map consisting of '0' and '1', which is used to record whether the pixels in NROI can be used for embedding information. When $M(i, j) = 0$ indicates that the pixel located in the i -row and the j -column may overflow after embedding information, so it cannot be used for embedding information. When $M(i, j) = 1$ indicates that this pixel can be used to embed information.

Step6 The square region additional information embedding

The additional information generated in **Step5** and **Step6** is embedded into the pixel LSB of the square region and then marked square region is obtained.

The marked ROI, the marked NROI and the marked square region together form the marked image.

2.4 Extraction and recovery algorithm

The seed pixels of the ROI and NROI do not change in the embedding algorithm, so it is very simple to restore the cover image. The concrete extraction and recovery process is as follows:

Step1 According to the default square area width h , the marked square region and marked non-square region are obtained.

Step2 According to the seed pixels of marked non-square region, the marked ROI and the marked NROI are divided by using the same segmentation method as for embedding.

Step3 According to the seed pixels in the marked non-square area, the AIA is adopted to recover the cover image except the square region.

Step4 Additional information is extracted from LSB in the marked square region to obtain ROI payload, ROI pixel maximum and minimum, NROI payload and NROI compressed location map, and the location map is decompressed to obtain the location map. At this time, the lowest bit in the square region is vacant.

Step5 The marked ROI information extraction

Comparing the changes of the non-seed pixels in the ROI with those in the marked ROI, then the extraction side performs the same changes in the ROI non-seed pixel stretch histogram to obtain the stretch histogram which determines the extraction sequence. According to the last peak bin of ROI extracted in the square area, the process of using CBHSR to extract information is described in Section 2.2. The concrete recovery of stretch histogram for determining the extraction order is as follows (13) and (14). I_R is ROI image, W_R is marked ROI image, SI is ROI image after non-seed pixel histogram stretch, SW is marked ROI image after non-seed pixel histogram stretch, and $I_R(2i, 2j)$, $W_R(2i, 2j)$, $SW(2i, 2j)$ and $SI(2i, 2j)$ are seed pixels, and that always remain unchanged. The rest are non-seed pixels.

$$\begin{cases} W_R(2i, 2j) = I_R(2i, 2j) \\ ee(2i + 1, 2j) = W_R(2i + 1, 2j) - I_R(2i + 1, 2j) \\ ee(2i, 2j + 1) = W_R(2i, 2j + 1) - I_R(2i, 2j + 1) \\ ee(2i + 1, 2j + 1) = W_R(2i + 1, 2j + 1) - I_R(2i + 1, 2j + 1) \end{cases} \tag{13}$$

$$\begin{cases} SW(2i, 2j) = SI(2i, 2j) \\ SW(2i + 1, 2j) = SI(2i + 1, 2j) + ee(2i + 1, 2j) \\ SW(2i, 2j + 1) = SI(2i, 2j + 1) + ee(2i, 2j + 1) \\ SW(2i + 1, 2j + 1) = SI(2i + 1, 2j + 1) + ee(2i + 1, 2j + 1) \end{cases} \tag{14}$$

It is worth noting that the extracted information is all embedded data in the last round of extraction, and other rounds contains 8-bit peak bin information.

Step6 The marked NROI information extraction

The prediction error expansion extraction is used for non-seed pixels in the marked NROI, and the concrete process is as follows:

- (1) Use the same predictor as the sender to predict x_i to get the predicted value x'_i .
- (2) The extended prediction error e'_i , where x''_i is the pixel value of the marked NROI.

$$e'_i = x''_i - x'_i \tag{15}$$

- (3) Restore the original prediction error value e_i .

$$e_i = \begin{cases} \lfloor \frac{e'_i}{2} \rfloor, & e'_i \in [-2T, 2T) \\ e'_i - T, & e'_i \in [2T, +\infty) \\ e'_i + T, & e'_i \in [-\infty, -2T) \end{cases} \tag{16}$$

- (4) Extract secret data.

$$b = \lfloor \frac{e'_i}{2} \rfloor, b \in \{0, 1\} \tag{17}$$

Step7 The information extracted from the marked ROI and the marked NROI is B , which is decrypted to obtain the secret information and the lowest bit of the square region.

Step8 The extracted lowest LSB of the square region is embedded into the square region with the lowest vacancy, and the recovered square region is obtained.

Step9 The recovered square region and recovered non-square region reconstructed cover image. The seed pixel is restored to get the input image.

2.5 Run-length compression algorithm and its improved algorithm

To save storage space, the NROI location map is compressed when it is embedded in square region. According to the size relationship between the location map and the square area,

RLE compression algorithm [2] or RLE improved compression algorithm is selected for compression. Because the size of the square area is fixed in advance, when the location map is still larger than the embeddable capacity provided by the square area after being compressed by RLE algorithm, the improved RLE algorithm is used.

(1) RLE compression algorithm

The principle of RLE compression algorithm is to use an attribute of blocks and a data block to represent a number of original continuous data strings. Because the location map is a binary image with a large number of continuous black and white pixels, the RLE is very suitable.

(2) RLE improved compression algorithm

RLE actually uses an 8-bit binary to represent a data block. To save space, the improved RLE uses a 5-bit binary when the data block is at [0,32] and uses an 8-bit binary when the data block is at (32,255]. Although a binary table is needed to represent the number of bits of data blocks, a large number of experimental results show that the compression rate of RLE improved algorithm is higher than that of RLE.

A simple example of RLE and its improved algorithm is shown in Fig. 9. To store a stream of data with a length of 434bits, RLE needs 81bits of storage space; RLE improved compression algorithm needs 78bits storage space. When there are more and more data in [0,32] in the data block, the advantages of improving the compression algorithm will become obvious.

3 Experimental results and discussion

In this section, MATLAB R2018b is used to simulate the algorithm and evaluate its performance in Windows 10 system with Intel (R) Core (TM) i5-7200u CPU @ 2.50GHz 2.70GHz. In order to better evaluate the performance of the algorithm, the medical image set [24] is selected for experimental testing. As shown in Fig. 10, a large number of experiments are conducted by selecting medical images of different sizes, different body parts and different types. Typical types of medical images include CT, MRI, CXR and X-ray. The experiment is mainly divided into two parts: discussing the performance of the proposed new AIA and discussing the performance of the proposed reversible information hiding scheme based on interpolation and histogram shift for medical images.

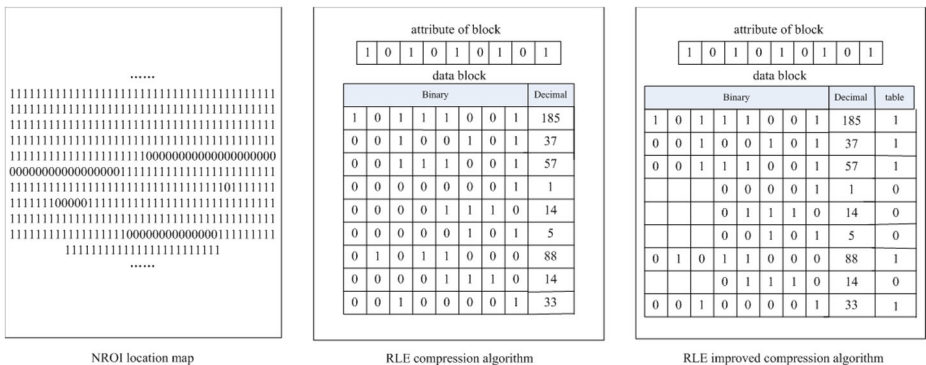


Fig. 9 Example of RLE and its improved algorithm

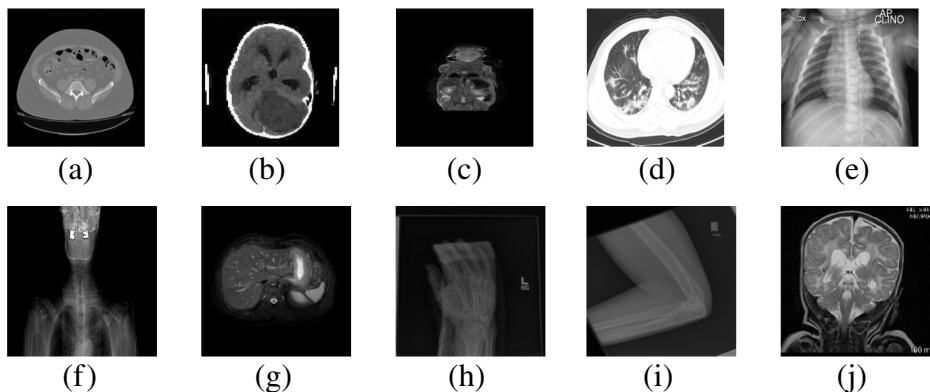


Fig. 10 Sample test image (a) Abdominal CT image, 256x256; (b) Brain MRI image, 180x180; (c) Pancreas MRI image, 256x256; (d) COVID-19 CT image, 720x541; (e) COVID-19 CXR image, 256x256; (f) Lung CT image, 888x 495; (g) Liver MRI image, 256x256; (h) Hand X-ray image, 406x512; (i) Leg X-ray image, 406x512; (j) Brain CT image, 180x180

3.1 The performance of proposed AIA

Firstly, the proposed AIA is compared with the image interpolation algorithm mentioned in Section 1. The performance evaluation indexes involved include information theory-based evaluation performance indexes: information entropy (EN) and cross entropy (C-EN), and image feature-based performance indexes: peak signal-to-noise ratio (PSNR), cross-correlation coefficient (NC)and average gradient (AG).

EN is an objective evaluation index to measure how much information an image contains. Assuming that i represents the gray value and $P(i)$ represents the probability of gray, the EN of the interpolated image (cover image) can be expressed by (18). The higher the EN, the richer the information content of the image and the better the image quality.

$$EN(I) = - \sum_i P_I(i) \log_I i \tag{18}$$

Cross-entropy reflects the difference between two images. The smaller the C-EN, the smaller the image difference. The difference between the interpolated image and the input image can be expressed by (19). Because the size of the input image is not equal to that of the interpolated image, the input image is first enlarged by using Nearest, that is, one pixel is changed into four pixels, and the image A1, which is the same size as the interpolated image, is obtained, and then compared.

$$C_EN(I, A1) = - \sum_i P_I(i) \log \frac{P_{A1}(i)}{P_I(i)} \tag{19}$$

PSNR is used to measure the ratio between effective information and noise in an image, which can reflect the image quality, such as whether it is distorted or not. The larger the PSNR value, the better the image quality. The PSNR of the interpolated image and the input image is compared. Assume that the interpolated image size is $M \times N$.

$$PSNR(I, A1) = 20 \log_{10} \frac{255}{\sqrt{MSE}} \tag{20}$$

$$MSE(I, A1) = \frac{1}{M \times N} \sum_{i=1}^M \sum_{j=1}^N (I(i, j) - A1(i, j))^2 \quad (21)$$

NC reflects the difference between two images, and the NC value is 1 when the images are the same. The NC between the interpolated image and the input image can be calculated by (22).

$$NC(I, A1) = \min \left(\sum_{i=1}^M \sum_{j=1}^N \frac{A1(i, j) \times I(i, j)}{I(i, j)^2}, \left(\sum_{i=1}^M \sum_{j=1}^N \frac{I(i, j)^2}{A1(i, j) \times I(i, j)} \right) \right) \quad (22)$$

AG reflect the tiny details and texture changes in an image on average, that is, the clarity of the image. The AG of the interpolated image can be calculated by (23). The larger the average gradient, the better the image quality.

$$AG(I) = \sum_{i=1}^M \sum_{j=1}^N \frac{\sqrt{(\Delta A1_x^2 \times \Delta A1_y^2) / 2}}{M \times N} \quad (23)$$

The ten images shown in Fig. 10 are respectively interpolated and expanded by different methods. Figure 11 shows the interpolated image obtained by the proposed interpolation algorithm, and it can be seen that the quality of the interpolated image is very good.

Table 1 shows the average values of various evaluation indexes obtained after ten images are processed by different interpolation algorithms. Because the Nearest method is adopted when the input image is set in equal size, its PSNR, NC and C-EN are especially good, which are ignored in comparison. Where, t stands for implementation time. It can be seen that the PSNR of the interpolated image obtained by the proposed AIA algorithm is 42.1805dB, which is higher than that of all methods except INP. The quality of the interpolated image is very good. The information entropy of the image obtained by the proposed method is higher than that of INP. Although the NC value of the interpolated image obtained by the proposed algorithm is lower than that of NMI method, its cross entropy is lower than that of NMI method, and its AG is higher than that of NMI method, which indicates that the difference between the interpolated image obtained by the proposed method and the original image after equal setting is smaller, and the definition of the interpolated image is better. Although the EN value of INMAP is higher than that of the proposed method, its PSNR is far lower than that of the interpolated image obtained by the proposed. Although the C-EN of the interpolated image obtained by Bicubic method is far less than that of the proposed method, its running time is very long, which has irreconcilable contradiction in the practical application of real-time medical field. In a word, it can be concluded that the comprehensive performance of the proposed interpolation algorithm AIA is optimal.

The pixels of the cover image can be divided into seed pixels and non-seed pixels by the AIA. One seed pixel corresponds to three non-seed pixels. We utilize non-seeded pixels for secret information embedding in the ROI, and the seed pixels remain unchanged. Theoretically, the number of available embedding pixels can be increased, thus the embedding capacity of the proposed scheme can be improved. It can also be seen from the experimental results that when the same embedding capacity is increased, the cover image obtained by the proposed AIA has good embedding quality compared with other interpolation methods. At the same time, the presence of seed pixels makes the restoration process of the cover image easy. In the detailed introduction of the proposed scheme in Section 2, it can be seen that the seed pixels and the histogram composed of non-seed pixels recovered from the seed pixels play an indispensable role in the extraction process of secret information. Without

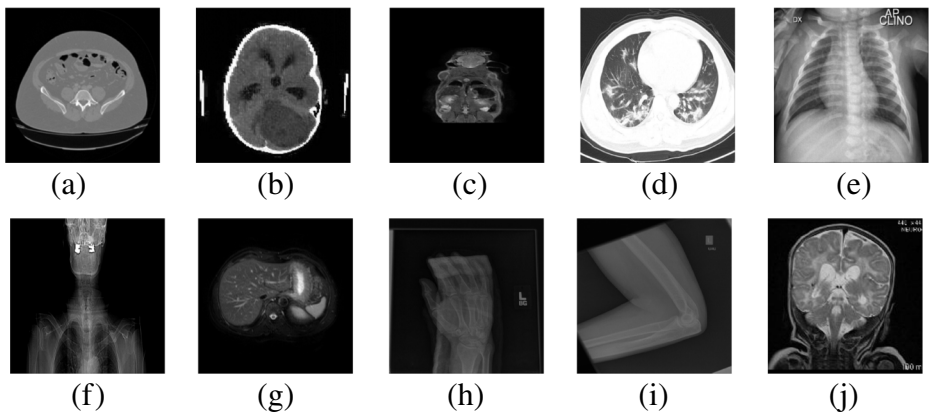


Fig. 11 Interpolated image (a) Abdominal CT image, 512x512; (b) Brain MRI image, 360x360; (c) Pancreas MRI image, 512x512; (d) COVID-19 CT image, 1440x1082; (e) COVID-19 CXR image, 512x512; (f) Lung CT image, 1776x990; (g) Liver MRI image, 512x512; (h) Hand X-ray image, 812x1024; (i) Leg X-ray image, 812x1024; (j) Brain CT image, 360x360

the reconstruction of the histogram, the determination of the extraction location cannot be successfully achieved, and thus the proposed reversible information hiding scheme cannot be successfully implemented completely.

3.2 The performance of proposed reversible information hiding scheme based on interpolation and histogram shift for medical images

The main purpose of a reversible information hiding scheme for medical images based on interpolation and histogram shift is to solve the damage to the imperceptibility of marked image caused by the use of histogram stretching to embed information. We use the stretched histogram as a tool for embedding location selection, embedding information at the corresponding locations of the original histograms. The method effectively avoids the large difference of pixel value at the same pixel point of the cover image and the marked image. Medical diagnosis has high requirements for medical images, and some slight changes may

Table 1 Comparison of interpolation algorithm performance (average of ten images)

	PSNR (dB)	NC	AG	EN	C-EN	t
Nearest [3]	Inf	1	2.6012	5.2838	0	0
Bilinear [3]	36.8633	0.9803	2.2102	5.3149	0.05503	4.182
Bicubic [3]	38.1216	0.9848	2.6000	5.2838	1.57E-05	15.226
INP [16]	46.9673	0.9973	2.3813	5.2956	0.00513	0.447
NMI [20]	42.0332	0.9936	2.2614	5.3045	0.00881	0.463
INMAP [14]	37.9777	0.9805	2.2064	5.3594	0.033633	0.511
AIA	42.1805	0.9918	2.2922	5.2969	0.00648	0.580

cause diagnostic errors. When we embed EPR and medical logo as secret information, we must ensure the subjective and objective quality of medical images to meet the actual needs of diagnosis while effectively protecting the privacy of patients and the rights and interests of hospitals. In proposed scheme, we use AIA to obtain seed pixels and non-seed pixels. Seed pixels reduce the complexity of the image restoration process. Non-seeded pixels ensure a balance between embedding capacity and embedding quality to a certain extent. The medical image shown in Fig. 10 is used as the result example to compare with the algorithm proposed by Yang et al. [37] and Gao et al. [10].

We compare the PSNR of the proposed algorithm with that of Yang’s and Gao’s algorithms using three images. The experimental results are shown in Fig. 12. After embedding different amounts of information in different images, the PSNR of the cover image and the marked image of the proposed method is always higher than that of the other two methods. This is because the algorithm proposed by Yang and Gao directly changes the pixel bin in the stretched histogram of the ROI region, so the difference in pixel values is large, and thus the PSNR value is low. The former stretches the ROI histogram within the range of [0,255], and the later determines the stretching range according to the histogram distribution of the ROI region in the image. In the proposed algorithm, the stretched histogram of ROI is used as a tool to select the embedding location of information. The information embedding is performed on the pixel bin of the original histogram of the ROI at the position corresponding to the ROI stretch histogram, so that the difference in pixel value changes is small, and the PSNR is greatly improved. To test this better, we also select six medical images such as Abdominal CT image, Brain MRI image, Pancreas MRI image, COVID-19 CXR image, Lung CT image and Brain CT image for histogram example as Figs. 13 and 14. The first row of each sub image is the ROI histogram of the cover image of Yang’s algorithm and Gao’s algorithm. The second and third row of each sub image is the ROI histogram of the marked image of Yang’s algorithm and Gao’s algorithm. The fourth row of each sub image is the ROI non-seed pixels histogram of the cover image of the proposed algorithm. The last row of each sub image is the ROI non-seed pixels histogram of the marked image of the proposed algorithm. The embedding rate of Abdominal CT image, Pancreas MRI image, COVID-19 CXR image and Lung CT image is 0.5 bpp. Brain MRI images and Brain CT images is 1bpp. The ROI histogram difference between before and after embedding information of the proposed scheme is obviously smaller than that of [10, 37]. In other words, the ROI histogram of the marked image is closer to that of the cover image in the proposed. The experimental results are consistent with our theoretical analysis.

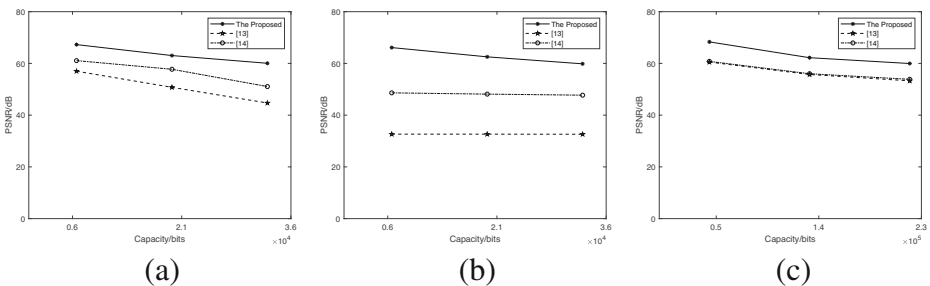


Fig. 12 Comparison of PSNR of [10, 37] and the proposed with different capacity in the Abdominal CT image, Pancreas MRI image and Lung CT image

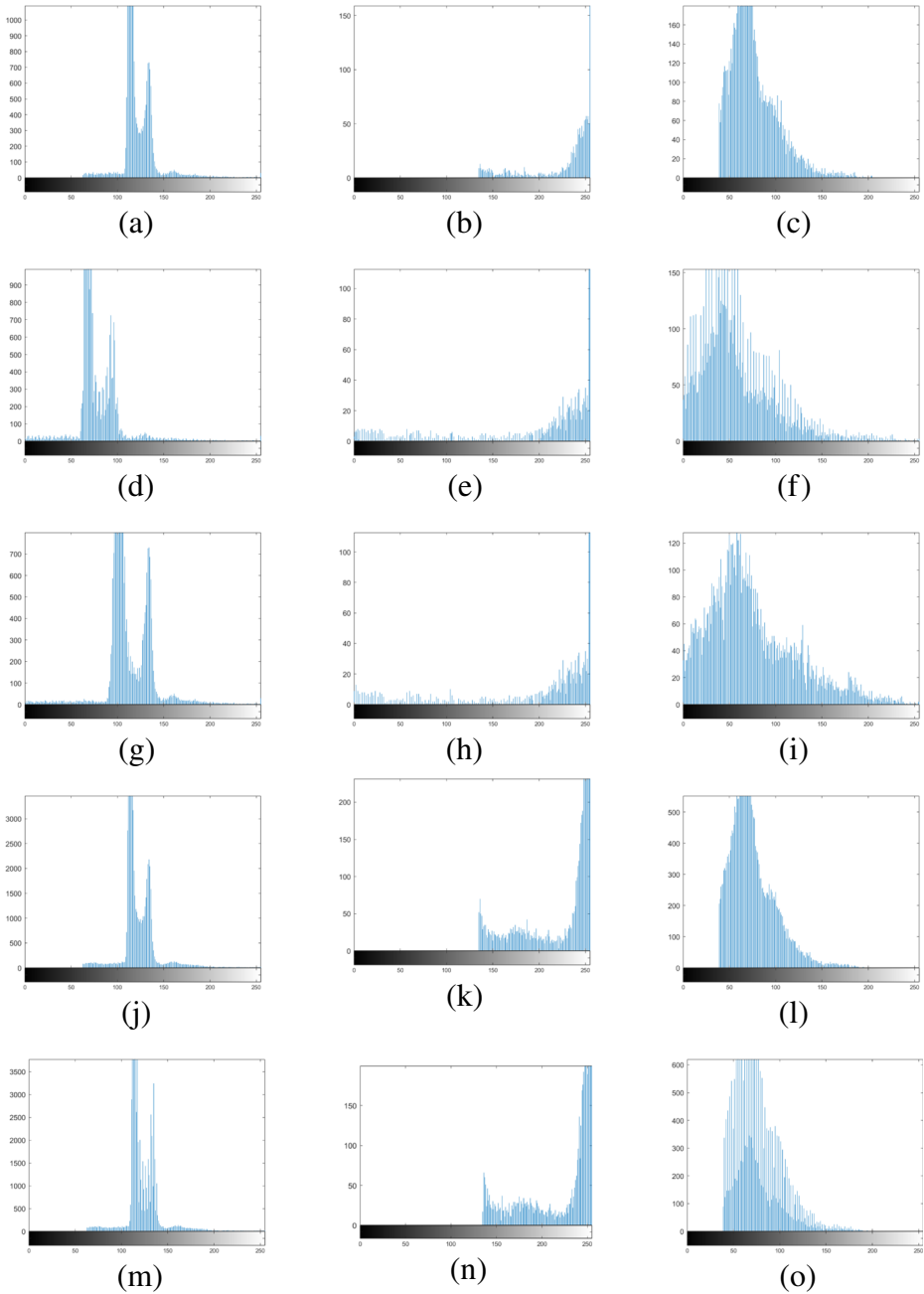


Fig. 13 Original and embedded histograms of Abdominal CT image, Brain MRI image and Pancreas MRI image in ROI by using three algorithms

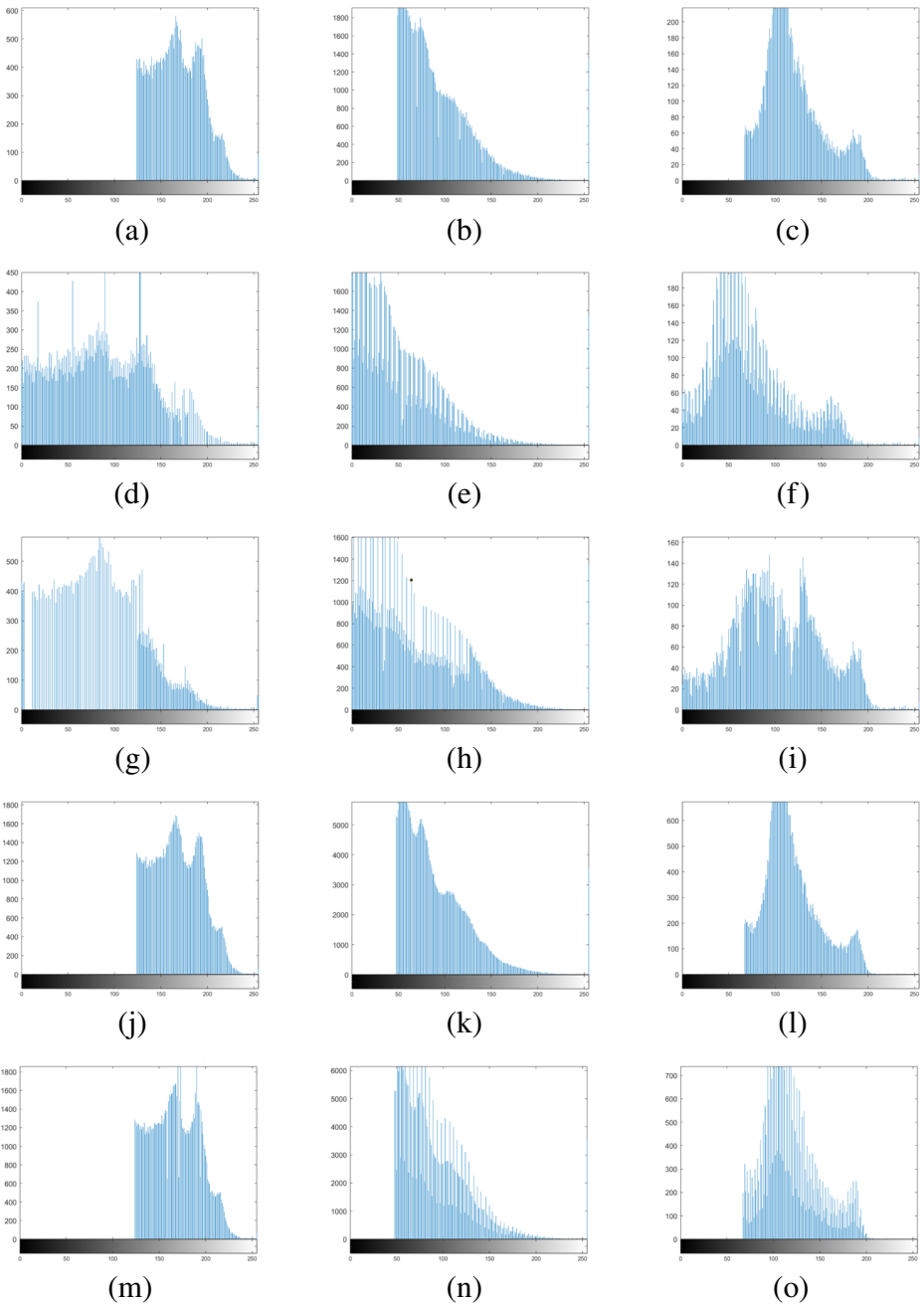


Fig. 14 Original and embedded histograms of COVID-19 CXR image, Lung CT image and Brain CT image in ROI by using three algorithms

In order to further reflect the superiority of the algorithm, two images are selected for detailed comparison of the three methods. Figures 15 and 16 show experimental results of two images obtained using the [10, 37], and the proposed method. The first column is the result using the algorithm of the [37], the second column is the result using the algorithm of the [10], and the third column is the result using the proposed algorithm. The embedding rates for the first and second rows in the figure are 0.3bpp and 0.5bpp respectively. The embedding rate of the first column of the third row is 0.7bpp, and the embedding rate of the last two columns is 1bpp. The embedding rate (bpp) is obtained by the ratio of the position of the embeddable information to the number of pixel points in the input image. The reason why the embedding rate of the 'Brain CT Image' test experiment does not reach 1bpp lies in the different embedding methods of the three algorithms. On the other hand, the perceptual enhancement degree of the marked image obtained by the former two algorithms depends on the degree of ROI histogram stretching, and their ROI embedding capacity also depends on the number of peak bin which its neighbor bin is absent in the ROI stretched histogram. However, the ROI embedding capacity of the proposed algorithm depends on the number of peak bin which its neighbor bin is absent obtained by the stretched histograms of ROI non-seeded pixels. Marked image obtained by using Yang and Gao algorithms has obvious changes, while the marked image obtained by the proposed

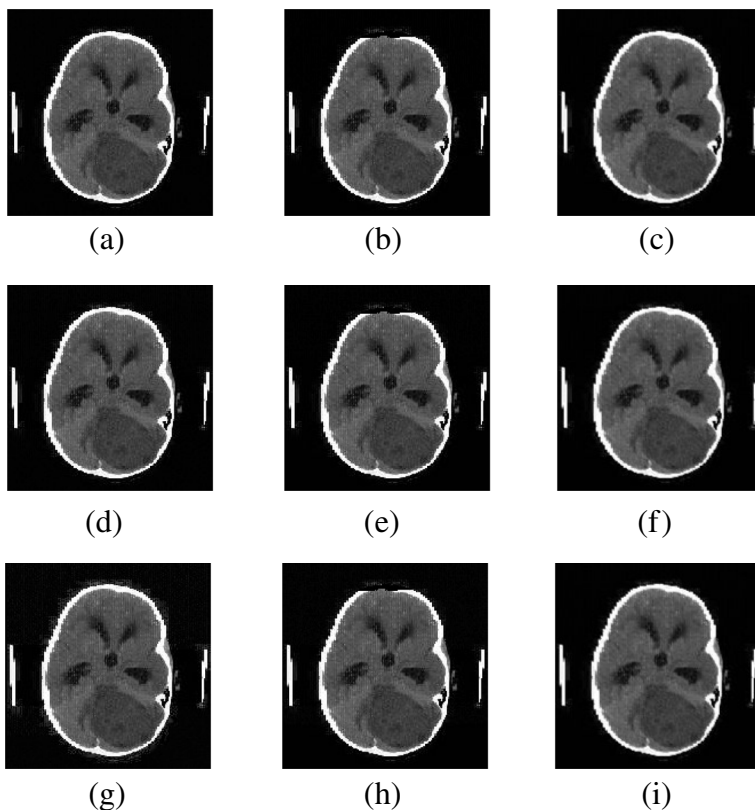


Fig. 15 Marked image of Brain MRI image by using three algorithms in 0.3bpp,0.5bpp,1bpp respectively

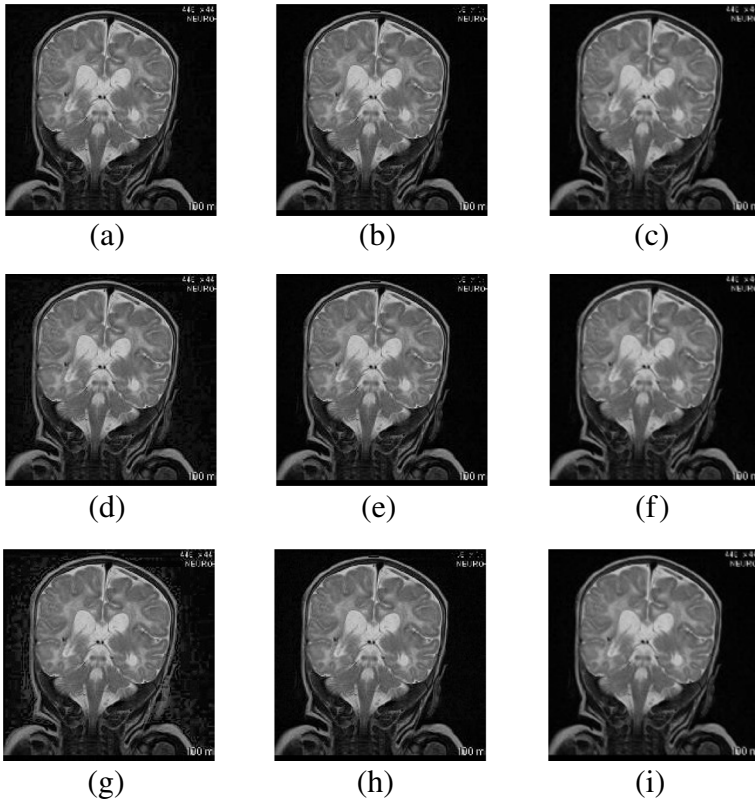


Fig. 16 Marked image of Brain CT image by using three algorithms in 0.3 bpp, 0.5bpp, 0.7 or 1bpp respectively

algorithm is hardly not changed in visual. Subjectively indicate that that proposed algorithm has better image quality. This can be felt more clearly in Figs. 16 and 17. Figure 17 is a marked image obtained by Pancreas MRI Image using Yang algorithm, Gao algorithm and the proposed algorithm respectively at an embedding rate of 0.5bpp.

In this section, the peak signal-to-noise ratio (PSNR), cross-correlation coefficient (NC), cross-entropy (C-EN), structural similarity (SSIM), Gini coefficient (G) and visual information fidelity for fusion (VIFF) are selected as metrics to evaluate the quality of the marked

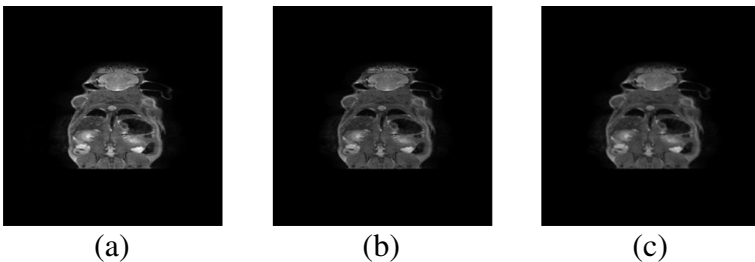


Fig. 17 Marked image of Pancreas MRI image by using three algorithms

Table 2 Evaluation results about marked image of Brain MRI image

Algorithm	Figure Number	bpp	PSNR	NC	SSIM	C-EN	G	VIFF
Yang [37]	Fig.15a	0.3	53.2681	0.9998	0.9866	0.2240	0.0001	0.9990
	Fig.15d	0.5	47.2767	0.9996	0.9607	0.2752	0.3500	0.9982
	Fig.15g	1	34.6670	0.9959	0.8055	0.8112	0.3500	0.9753
Gao [10]	Fig.15b	0.3	60.7005	0.9547	0.9795	0.1138	0.0001	0.9241
	Fig.15e	0.5	52.6848	0.9548	0.9730	0.1493	0.0054	0.9235
	Fig.15h	1	43.5552	0.9551	0.9181	0.2916	0.3138	0.9212
The Proposed	Fig.15c	0.3	62.4598	0.9999	0.9989	0.0331	0.0008	0.9999
	Fig.15f	0.5	59.2434	0.9997	0.9986	0.0592	0.0013	0.9998
	Fig.15i	1	54.4413	0.9996	0.9968	0.0791	0.0122	0.9994

images. Structural similarity (SSIM) [13] compares the differences between the cover image and the marked

image in brightness, contrast, and structure, respectively. SSIM is accordant to the human eye's judgment on image quality and can objectively measure the degree of similarity between images. SSIM value is 1 when two images are consistent. Gini Coefficient (G) [7] is an indicator to select the optimal features when decision trees are used for classification problems in machine learning. We divide the pixels of the marked image into two categories. The first category is that only the lowest pixel is modified and the pixel is not modified. All except the first category were the second category. When the G is smaller, the purity of the data set is higher, that is, the quality of the marked image is better. VIFF [12] is a proposed index to measure the quality of fused images based on visual information fidelity. The larger the value

of VIFF, the better the quality of the marked image. The PSNR, NC, C-EN, SSIM, G and VIFF values for the 'Brain MRI Image' and 'Brain CT Image' marked images at 0.3bpp, 0.5bpp, and 1bpp or 0.7bpp embedding rates are presented in Tables 2 and 3. In order to be more convincing, We also select more images from [24] and average evaluation results of thirty medical images presented in Table 4. It can be observed that the PSNR of the proposed method is very high and has been maintained above 50dB. The PSNR is improved by above 25% compared to [10] at 1bpp and improved by above 50% compared to

Table 3 Evaluation results about marked image of Brain CT image

Algorithm	Figure Number	bpp	PSNR	NC	SSIM	C-EN	G	VIFF
Yang [37]	Fig.16a	0.3	40.8996	0.9986	0.9547	0.1937	0.3648	0.9817
	Fig.16d	0.5	33.7813	0.9966	0.8820	0.2565	0.4473	0.9572
	Fig.16g	0.7	32.1935	0.9918	0.8025	0.3389	0.4481	0.9033
Gao [10]	Fig.16b	0.3	58.5705	0.9945	0.9943	0.0220	0.0001	0.9943
	Fig.16e	0.5	51.1226	0.9946	0.9889	0.0404	0.1666	0.9920
	Fig.18h	1	42.6315	0.9952	0.9572	0.1947	0.3378	0.9835
The Proposed	Fig.16c	0.3	56.3166	0.9999	0.9994	0.0115	0.0053	0.9995
	Fig.16f	0.5	55.2731	0.9993	0.9992	0.0382	0.0054	0.9993
	Fig.16i	1	51.9115	0.9992	0.9977	0.0507	0.0144	0.9984

Table 4 Average evaluation results of thirty of marked images from [34]

Algorithm	bpp	PSNR	NC	SSIM	C-EN	G	VIFF
Yang [37]	0.3	39.0304	0.9428	0.9914	0.1371	0.1421	0.9892
	0.5	35.4121	0.9414	0.9669	0.2894	0.3035	0.9735
	0.7	34.4489	0.9387	0.8986	0.4165	0.4244	0.9301
Gao [10]	0.3	55.3313	0.9961	0.9875	0.1571	0.0039	0.9970
	0.5	51.1539	0.9961	0.9809	0.1961	0.0934	0.9956
	1	44.9662	0.9962	0.9202	0.3139	0.3290	0.9895
The Proposed	0.3	59.4126	0.9991	0.9998	0.0124	0.0023	0.9995
	0.5	57.5278	0.9987	0.9990	0.0389	0.0022	0.9993
	1	56.5278	0.9986	0.9964	0.0766	0.0103	0.9992

Yang et al. [37] at the higher embedding rate. With the increase of the embedding rate, the difference between the PSNR of the proposed method and other two methods is larger and larger. It shows that the proposed method can guarantee the high quality of the marked image with high embedding capacity. The SSIM, NC and VIFF values obtained by using the proposed algorithm are also very high and can be kept around 0.999. The cross entropy of cover image and marked image

is much less than that of the two comparison algorithms in the same case. The experimental objectively indicates that the proposed algorithm has better image quality. Experimental results show that the algorithm not only achieves information protection, but also meets the needs of medical image diagnosis.

4 Conclusion

In this paper, a new reversible information hiding scheme based on interpolation and histogram shift for medical images is proposed. We obtain seeded and non-seeded pixels by using the proposed AIA. Seed pixels reduce the complexity of the image restoration process. The non-seeded pixels avoid the risk of potentially causing a decrease in embedding capacity when using stretched histograms as a location selection tool and balance the embedding quality and embedding capacity. According to the characteristics of medical images, the regions of the images are divided, and the CBHSR is used in the ROI. The information is embedded in the pixel bin of the original histogram corresponding to stretch histogram instead of directly embedded in the ROI stretched histogram, which effectively avoids the problem of visual perception.

We selected different sizes, body parts and types of medical images for the experiment. Experimental results show that the proposed algorithm maintains the similarity and imperceptibility of the cover image and the marked image compared with the comparison algorithms. While ensuring the embedding capacity, the PSNR of the proposed scheme is increased to about 50dB at the same embedding rate, which is improved by above 25% compared to [10] at 1bpp and the SSIM, NC and VIFF are kept at 0.99, which provides the best image quality based on subjective and objective. When we embed EPR and medical

logo into medical images as secret information, it not only effectively protects the privacy of patients and the rights and interests of hospitals, but also meets the actual requirements of image quality when medical images are used for diagnosis.

In the subsequent study, the polygon fitting method will be considered for more refined segmentation of medical images when dividing ROI and NROI to further improve the performance of the algorithm. In the future, we will also consider designing histogram stretching rules, and combine the adaptive stretching histogram method with the proposed method, as well as integrating machine learning, so as to enhance the robustness and algorithm security, so that it can be better applied to the medical field.

Acknowledgements This paper was supported by the National Nature Science Foundation of China (Program No. 62202377), the Natural Science Basic Research Plan of Shaanxi Province of China (Program No. 2021JM-463, 2022JM-353), the Graduate Innovation Fund of Xi'an University of Posts and Telecommunications (CXJJDL2022015).

Data Availability All data generated or analysed during this study are included in this published article.

The datasets generated during and/or analysed during the current study are available from the corresponding author on reasonable request.

Declarations

Conflict of Interests The authors declare that they have no conflict of interest.

Authors are responsible for correctness of the statements provided in the manuscript.

References

1. Abadi MAM, Danyali H, Helfroush MS (2010) Reversible watermarking based on interpolation error histogram shifting. Paper presented at the 5th international symposium on Telecommunications, Kish Island, Iran, 850–854 Dec 2010
2. Al-nuaimi AHH, Al-juboori SS, Mohammed RJ (2017) Image compression using proposed enhanced run length encoding algorithm. *Ibn AL-haitham J Pure Appl Sci*, vol 24(1)
3. Ashraf I, Hur S, Park Y (2017) An investigation of interpolation techniques to generate 2d intensity image from LIDAR data. *IEEE Access* 5:8250–8260. <https://doi.org/10.1109/ACCESS.2017.2699686>
4. Avinashiappan A, Mayilsamy B, Hemant J (2022) Security enhanced roi based reversible watermarking for medical images. *DYNA-Ingeniería e Industria* 97(2):210–216. <https://doi.org/10.1109/TNSE.2021.3139671>
5. Bamal R, Kasana SS (2019) Dual hybrid medical watermarking using walsh-slantlet transform. *Multimed Tools Appl* 78(13):17899–17927. <https://doi.org/10.1007/s11042-018-6820-9>
6. Bhardwaj R (2021) Hiding patient information in medical images: an enhanced dual image separable reversible data hiding algorithm for E-healthcare. *J Ambient Intell Humanized Comput*:1–17. <https://doi.org/10.1007/s12652-021-03299-2>
7. Chauhan SAAK, Singh M (2021) Data science and data analytics: artificial intelligence and machine learning integrated based approach. *Data Sci Data Anal Opportunities Challenges*, vol 1. <https://doi.org/10.1109/TNSE.2021.3139671>
8. Dewangan P, Paikaray BK, Swain D, Chakravarty S (2021) Reversible region-based embedding in images for secured telemedicine approach. Springer, pp 545–554. https://doi.org/10.1007/978-981-33-4859-2_53
9. Gao G, Shi Y (2015) Reversible data hiding using controlled contrast enhancement and integer wavelet transform. *IEEE Signal Process Lett* 22(11):2078–2082. <https://doi.org/10.1109/LSP.2015.2459055>
10. Gao G, Tong S, Xia Z (2021) Reversible data hiding with automatic contrast enhancement for medical images. *Signal Process* 178:107817. <https://doi.org/10.1016/j.sigpro.2020.107817>
11. Geetha R, Geetha S (2020) Embedding electronic patient information in clinical images: an improved and efficient reversible data hiding technique. *Multimed Tools Appl* 79(19–20):12869–12890. <https://doi.org/10.1007/s11042-019-08484-2>
12. Han Y, Cai Y, Cao Y, Xu X (2013) A new image fusion performance metric based on visual information fidelity. *Inf Fusion* 14(2):127–135. <https://doi.org/10.1016/j.inffus.2011.08.002>

13. Hore A, Ziou D (2010) Image quality metrics: PSNR vs. SSIM. In: Paper presented at the 20th international conference on pattern recognition, pp 2366–2369 2010
14. Hu J, Li T (2015) Reversible steganography using extended image interpolation technique. *Comput Electr Eng* 46:447–455. <https://doi.org/10.1016/j.compeleceng.2015.04.014>
15. Hurrah NN, Parah SA, Sheikh JA (2020) Embedding in medical images: an efficient scheme for authentication and tamper localization. *Multimed Tools Appl* 79(29–30):21441–21470. <https://doi.org/10.1007/s11042-020-08988-2>
16. Jung K, Yoo K (2009) Data hiding method using image interpolation. *Comput Standards Interfaces* 31(2):465–470. <https://doi.org/10.1016/j.csi.2008.06.001>
17. Kapadia NAM (2022) A review: reversible information hiding and bio-inspired optimization. *Artif Intell Technol*:489–506. https://doi.org/10.1007/978-981-16-6448-9_48
18. Khosravi MR, Yazdi M (2018) A lossless data hiding scheme for medical images using a hybrid solution based on IBRW error histogram computation and quartered interpolation with greedy weights. *Neural Comput Appl* 30(7):2017–2028. <https://doi.org/10.1007/s00521-018-3489-y>
19. Lee H (2019) Adaptive reversible watermarking for authentication and privacy protection of medical records. *Multimed Tools Appl* 78(14):19663–19680. <https://doi.org/10.1007/s11042-019-7322-0>
20. Lee C, Huang Y (2012) An efficient image interpolation increasing payload in reversible data hiding. *Expert Syst Appl* 39(8):6712–6719. <https://doi.org/10.1016/j.eswa.2011.12.019>
21. Liao X, Yin J, Chen M, Qin Z (2022) Adaptive payload distribution in multiple images steganography based on image texture features. *IEEE Trans Dependable Secure Comput* 19(2):897–911. <https://doi.org/10.1109/TDSC.2020.3004708>
22. Liao X, Yu Y, Li B, Li Z, Qin Z (2022) A new payload partition strategy in color image steganography. *IEEE Trans Circuits Syst Video Technol* 30(3):685–696. <https://doi.org/10.1109/TCSVT.2019.2896270>
23. Liu X, Lou J, Fang H, Chen Y (2019) A novel robust reversible watermarking scheme for protecting authenticity and integrity of medical images. *IEEE Access* 7:76580–76598. <https://doi.org/10.1109/ACCESS.2019.2921894>
24. Linhandev (2020). Medical images dataset. <https://github.com/linhandev/dataset>
25. Loan NA, Parah SA (2017) Hiding electronic patient record (EPR) in medical images: a high capacity and computationally efficient technique for e-healthcare applications. *J Biomed Inf* 73:125–136. <https://doi.org/10.1016/j.jbi.2017.08.002>
26. Mata-Mendoza D (2021) An improved roi-based reversible data hiding scheme completely separable applied to encrypted medical images. *Health Technol* 11(4):835–850. <https://doi.org/10.1007/s12553-021-00562-6>
27. Ni Z, Shi YQ, Ansari N, Su W (2006) Reversible data hiding. *IEEE Trans Circuits Syst Vid Technol* 16(3):354–362. <https://doi.org/10.1109/TCSVT.2006.869964>
28. Otsu N (1979) A threshold selection method from gray-level histograms. *IEEE Trans Syst Man Cybern* 9(1):62–66. <https://doi.org/10.1109/TSMC.1979.4310076>
29. Sachnev V, Kim H (2009) Reversible watermarking algorithm using sorting and prediction. *IEEE Trans Circuits Syst Video Technol* 19(7):989–999. <https://doi.org/10.1109/TCSVT.2009.2020257>
30. Selvam P (2017) Hybrid transform based reversible watermarking technique for medical images in telemedicine applications. *Optik* 145:655–671. <https://doi.org/10.1016/j.ijleo.2017.07.060>
31. Sh YQ (2004) Reversible data hiding. Springer, pp 1–12. https://doi.org/10.1007/978-3-540-31805-7_1
32. Showkat S, Parah SA, Gull S (2021) Embedding in medical images with contrast enhancement and tamper detection capability. *Multimed Tools Appl* 80(2):2009–2030. <https://doi.org/10.1007/s11042-020-09732-6>
33. Tan J, Liao X, Liu J, Cao Y, Jiang H (2022) Channel attention image steganography with generative adversarial networks. *IEEE Trans Netw Sci Eng* 9(2):888–903. <https://doi.org/10.1109/TNSE.2021.3139671>
34. Thodi DM, J J (2004) Prediction-error based reversible watermarking. *IEEE*, pp 1549–1552. <https://doi.org/10.1109/ICIP.2004.1421361>
35. Tian J (2003) Reversible data embedding using a difference expansion. *IEEE Trans Circuits Syst Vid Technol* 13(8):890–896. <https://doi.org/10.1109/TCSVT.2003.815962>
36. Wu H, Dugelay J, Shi Y (2015) Reversible image data hiding with contrast enhancement. *IEEE Signal Process Lett* 22(1):81–85. <https://doi.org/10.1109/LSP.2014.2346989>
37. Yang Y, Zhang W, Liang D, Yu N (2018) A roi-based high capacity reversible data hiding scheme with contrast enhancement for medical images. *Multimed Tools Appl* 77(14):18043–18065. <https://doi.org/10.1007/s11042-017-4444-0>

Publisher's note Springer Nature remains neutral with regard to jurisdictional claims in published maps and institutional affiliations.

Springer Nature or its licensor (e.g. a society or other partner) holds exclusive rights to this article under a publishing agreement with the author(s) or other rightsholder(s); author self-archiving of the accepted manuscript version of this article is solely governed by the terms of such publishing agreement and applicable law.